

## 7 COMPARISON

### 7.1 STRUCTURE

#### 7.1.1 Introduction

The comparison between the results of the proposed algorithms must be carried on using a common structure. In order to have significant results the structure should be a realistic one, which means a structure not designed to withstand earthquakes, or at least designed with outdated codes. If possible moreover, the structural scheme should be a widespread one, so that the research studies on passive/active control can be applied in the retrofitting of a real structure, and, in case a real seismic event happens, verified. Finally the computational model should be clear and results, at least the linear ones, should be easily reproducible. This last feature leads to the possibility for a wider comparison with other studies.

The problem to have common models with which comparing different methods of retrofitting, that is define benchmark structures, arose since the middle of the nineties. The American Society of Civil Engineers (ASCE) Committee on Structural Control developed in 1997 a benchmark study, focused primarily on the comparison of structural control algorithms for three-story building models. Several of the studied algorithms have been also experimentally verified. In 2004 a new generation of benchmark control problem, firstly designed for phase II of the SAC steel project, was presented. It is composed by 3-, 9- and 20-story buildings, firstly designed by Brandow & Johnson Associates (1996). Although not actually constructed, these structures meet seismic code and represent typical low-, medium- and high-rise buildings. These building were chosen because, serving as benchmark structures for the SAC project, a wider base for the comparison of results is available.

In the present research the 9-story building has been chosen, due to its characteristics are in between the three structures. Moreover a modification of it is considered in order to evaluate the efficiency of the methods also for irregular structures.

The specifications for the two selected buildings are discussed in the following paragraphs.

#### 7.1.2 Regular building

The nine-story benchmark structure is 45.73 m by 45.73 m in plan, and 37.19 m in elevation. The bays are 9.15 m on center, in both directions, with five bays each. The building scheme follows in other well known structures used in California. It consists on an external moment resisting frame which contains a pinned framing. The lateral load resisting system of the building is comprised of steel perimeter moment resisting frames.

The interior bays of the structure contain simple framing which carries vertical loads only and it is assumed that it doesn't offer any resistance to horizontal forces. This structural scheme was well appreciated by architects because of the relatively absence of high obstacles in the design of internal spaces. Although from an engineering point of view this practice doesn't follow the principle of redundancy which states that structures must have the highest number of defense lines against seismic actions. For this reason this structural scheme didn't meet success.

In details the columns are 345 MPa steel. The interior columns of the moment resisting frame are wide flange while the corner ones are box columns. The levels of the building are numbered from with respect to the ground level. The ninth level is the roof and the basement level is denoted as B-1. Typical floor-to-floor heights (measured from center of beam to center of beam) are 3.96 m. The basement one is 3.65 m while the first floor is 5.49 m. As it is possible to see while the regularity on plant is guaranteed, in elevation there is a slight irregularity in the first floor: the increased height is about the 38%. This characteristic reflects the necessity to have at the first floors wider spaces to lodge activities different from residential ones.

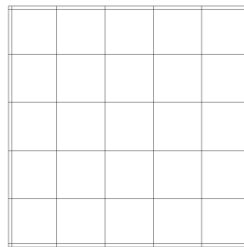


Figure 7.1-1 Plant of the structure

The column lines employ two-tier construction, i.e. monolithic column pieces are connected every two levels beginning with the first level. Column splices, which are seismic splices to carry bending forces, are located, for sake of simplicity, in correspondence to the beam-column nodes. The column bases are modeled as pinned to the ground. Concrete foundation walls and surrounding soil are assumed to restrain the structure at the ground level from horizontal displacements.

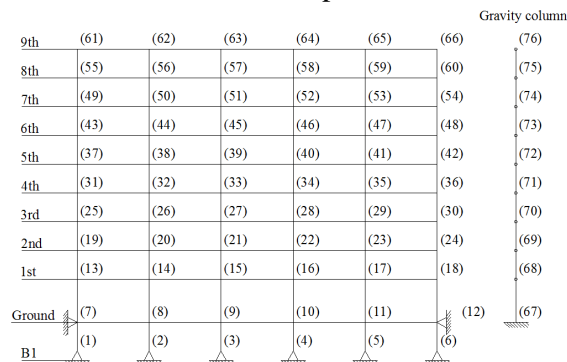


Figure 7.1-2 Elevation view

The floors are composite construction (i.e., concrete and steel). The floor system is comprised of 248 MPa steel wide flange beams acting compositely with the floor slab. In accordance with common practice the floor system, which provides diaphragm action, is assumed to be rigid in the horizontal plane. The inertial effects of each level are assumed to be carried by the floor diaphragm to each perimeter moment resisting frame, hence, each frame resists one-half of the entire mass associated with the entire structure.

The seismic mass of the structure is due to various components of the structure, both structural and non-structural, including the steel framing, floor slabs, flooring and roofing. As explained in chapter 2.2.2, in order to consider geometric nonlinearities, vertical weights and loads associated with the inner part of the structure are considered in the so called gravity column (nodes 67-76). The seismic weights and the static loads are summarized in Table 7.1-1 and Table 7.1-2:

**Table 7.1-1 Seismic weights in [kN]**

<b>Node</b>	<b>X-</b>	<b>Y-</b>	<b>Node</b>	<b>X-</b>	<b>Y-</b>	<b>Node</b>	<b>X-</b>	<b>Y-</b>	<b>Node</b>	<b>X-</b>	<b>Y-</b>
<b>1</b>	0.0	0.0	<b>19</b>	0.0	98.9	<b>37</b>	0	98.9	<b>55</b>	0	98.9
<b>2</b>	0.0	0.0	<b>20</b>	0.0	197.8	<b>38</b>	0	197.8	<b>56</b>	0	197.8
<b>3</b>	0.0	0.0	<b>21</b>	0.0	197.8	<b>39</b>	0	197.8	<b>57</b>	0	197.8
<b>4</b>	0.0	0.0	<b>22</b>	0.0	197.8	<b>40</b>	0	197.8	<b>58</b>	0	197.8
<b>5</b>	0.0	0.0	<b>23</b>	0.0	197.8	<b>41</b>	0	197.8	<b>59</b>	0	197.8
<b>6</b>	0.0	0.0	<b>24</b>	0.0	98.9	<b>42</b>	0	98.9	<b>60</b>	0	98.9
<b>7</b>	0.0	96.5	<b>25</b>	0.0	98.9	<b>43</b>	0	98.9	<b>61</b>	0	107
<b>8</b>	0.0	193.0	<b>26</b>	0.0	197.8	<b>44</b>	0	197.8	<b>62</b>	0	214
<b>9</b>	0.0	193.0	<b>27</b>	0.0	197.8	<b>45</b>	0	197.8	<b>63</b>	0	214
<b>10</b>	0.0	193.0	<b>28</b>	0.0	197.8	<b>46</b>	0	197.8	<b>64</b>	0	214
<b>11</b>	0.0	193.0	<b>29</b>	0.0	197.8	<b>47</b>	0	197.8	<b>65</b>	0	214
<b>12</b>	0.0	96.5	<b>30</b>	0.0	98.9	<b>48</b>	0	98.9	<b>66</b>	0	107
<b>13</b>	0.0	101.0	<b>31</b>	0.0	98.9	<b>49</b>	0	98.9	<b>67</b>	0	0
<b>14</b>	0.0	202.0	<b>32</b>	0.0	197.8	<b>50</b>	0	197.8	<b>68</b>	5050	4040
<b>15</b>	0.0	202.0	<b>33</b>	0.0	197.8	<b>51</b>	0	197.8	<b>69</b>	4945	3956
<b>16</b>	0.0	202.0	<b>34</b>	0.0	197.8	<b>52</b>	0	197.8	<b>70</b>	4945	3956
<b>17</b>	0.0	202.0	<b>35</b>	0.0	197.8	<b>53</b>	0	197.8	<b>71</b>	4945	3956
<b>18</b>	0.0	101.0	<b>36</b>	0.0	98.9	<b>54</b>	0	98.9	<b>72</b>	4945	3956
									<b>73</b>	4945	3956
									<b>74</b>	4945	3956
									<b>75</b>	4945	3956
									<b>76</b>	5350	4280

**Table 7.1-2 Static loads in [kN]**

<b>Node ID</b>	<b>Y-load</b>	<b>Node ID</b>	<b>Y-load</b>	<b>Node ID</b>	<b>Y-load</b>	<b>Node ID</b>	<b>Y-load</b>
<b>1</b>	0.0	<b>19</b>	-98.9	<b>37</b>	-98.9	<b>55</b>	-98.9
<b>2</b>	0.0	<b>20</b>	-197.8	<b>38</b>	-197.8	<b>56</b>	-197.8

<b>3</b>	0.0	<b>21</b>	-197.8	<b>39</b>	-197.8	<b>57</b>	-197.8
<b>4</b>	0.0	<b>22</b>	-197.8	<b>40</b>	-197.8	<b>58</b>	-197.8
<b>5</b>	0.0	<b>23</b>	-197.8	<b>41</b>	-197.8	<b>59</b>	-197.8
<b>6</b>	0.0	<b>24</b>	-98.9	<b>42</b>	-98.9	<b>60</b>	-98.9
<b>7</b>	-101.0	<b>25</b>	-98.9	<b>43</b>	-98.9	<b>61</b>	-107
<b>8</b>	-202.0	<b>26</b>	-197.8	<b>44</b>	-197.8	<b>62</b>	-214
<b>9</b>	-202.0	<b>27</b>	-197.8	<b>45</b>	-197.8	<b>63</b>	-214
<b>10</b>	-202.0	<b>28</b>	-197.8	<b>46</b>	-197.8	<b>64</b>	-214
<b>11</b>	-202.0	<b>29</b>	-197.8	<b>47</b>	-197.8	<b>65</b>	-214
<b>12</b>	-101.0	<b>30</b>	-98.9	<b>48</b>	-98.9	<b>66</b>	-107
<b>13</b>	-98.9	<b>31</b>	-98.9	<b>49</b>	-98.9	<b>67</b>	0
<b>14</b>	-197.8	<b>32</b>	-197.8	<b>50</b>	-197.8	<b>68</b>	-9090
<b>15</b>	-197.8	<b>33</b>	-197.8	<b>51</b>	-197.8	<b>69</b>	-8901
<b>16</b>	-197.8	<b>34</b>	-197.8	<b>52</b>	-197.8	<b>70</b>	-8901
<b>17</b>	-197.8	<b>35</b>	-197.8	<b>53</b>	-197.8	<b>71</b>	-8901
<b>18</b>	-98.9	<b>36</b>	-98.9	<b>54</b>	-98.9	<b>72</b>	-8901
						<b>73</b>	-8901
						<b>74</b>	-8901
						<b>75</b>	-8901
						<b>76</b>	-9630

The sizes of beams and columns decrease with the height. The scheme of the member section is shown below.

Table 7.1-3 Member sections

Beams		Columns	
Ground-2nd level	W36x160	Ground-1st level	W14x500
3rd-6th level	W36x135	2nd-3rd level	W14x455
7th level	W30x99	4rd-5th level	W14x370
8th level	W27x84	6th-7th level	W14x283
9th level	W24x62	8th-9th level	W14x257

The modeling of the structure requires the definition of both elastic and plastic properties of each element. The cross-sectional area  $A_x$ , the shear area  $A_y$  and the moment of inertia  $I_{zz}$  provide the information on the elastic behavior and are summarized Table 7.1-4.

Table 7.1-4 Elastic properties of members

Section ID	d [mm]	$A_x$ [mm <sup>2</sup> ]	$A_y$ [mm <sup>2</sup> ]	$I_{zz}$ [mm <sup>4</sup> ]
<b>W30x99</b>	753.11	1.88E+04	9.95E+03	1.66E+09
<b>W27x84</b>	678.434	1.60E+04	7.93E+03	1.19E+09

<b>W24x62</b>	602.742	1.30E+04	6.35E+03	7.62E+08
<b>W36x160</b>	914.654	3.03E+04	1.51E+04	4.06E+09
<b>W36x135</b>	902.97	2.56E+04	1.38E+04	3.25E+09
<b>W14x500</b>	497.84	9.48E+04	2.77E+04	3.42E+09
<b>W14x455</b>	483.108	8.65E+04	2.69E+04	2.99E+09
<b>W14x370</b>	455.168	7.03E+04	1.91E+04	2.26E+09
<b>W14x283</b>	425.196	5.37E+04	1.39E+04	1.60E+09
<b>W14x257</b>	416.052	4.88E+04	1.24E+04	1.42E+09

Inelastic properties consist essentially in the definition of the behavior of the plastic hinges. In the present analysis the bilinear hysteretic rule has been considered using a bilinear factor of 0.02 while the length of the hinge has been taken for sake of simplicity equal to the depth of the member.

The parameters that define the hysteretic behavior are different in case of beam or column elements. In presence of columns in fact the interaction between axial and bending forces modifies the values of yielding actions. Hence interaction diagrams must be defined and, in this analysis, a linear relationship has been considered. The values of yielding moments and, in the case of columns, yielding axial forces are reported in Table 7.1-5.

Table 7.1-5 Inelastic properties of members

<b>Section ID</b>	<b>fy [Mpa]</b>	<b>Zzz [mm<sup>3</sup>]</b>	<b>Mpl[kNmm]</b>	<b>Py [kN]</b>
<b>W30x99</b>	248	5.11E+06	1.27E+06	--
<b>W27x84</b>	248	4.00E+06	9.92E+05	--
<b>W24x62</b>	248	2.90E+06	7.19E+05	--
<b>W36x160</b>	248	1.02E+07	2.54E+06	--
<b>W36x135</b>	248	8.34E+06	2.07E+06	--
<b>W14x500</b>	345	1.72E+07	5.94E+06	3.27E+04
<b>W14x455</b>	345	1.53E+07	5.29E+06	2.98E+04
<b>W14x370</b>	345	1.21E+07	4.16E+06	2.43E+04
<b>W14x283</b>	345	8.88E+06	3.06E+06	1.85E+04
<b>W14x257</b>	345	7.98E+06	2.75E+06	1.68E+04

The most part of the methods analyzed require the stiffness matrix. This matrix can be computed for the linear case using the force method considering one degree of freedom for each level. Thus a unit force is applied iteratively at all story, and the values of all the floor displacements are recorded in vectors. The flexibility matrix is composed by these vectors and its inversion gives the rigidity matrix. All the results of the linear comparison are obtained using this matrix which is reported in Table 7.1-6.

**Table 7.1-6 Stiffness matrix of the nine-story building**

702,489.1	-562,455.2	120,330.8	-14,580.1	781.1	-255.9	-76.5	941.6	-421.2
-562,455.2	945,528.3	-570,334.9	122,475.7	-11,391.5	1,544.8	-90.1	-1,624.5	986.1
120,330.8	-570,334.9	898,069.5	-530,294.8	101,309.2	-11,953.8	1,577.8	1,145.4	-854.3
-14,580.1	122,475.7	-530,294.8	786,776.7	-442,977.7	85,401.3	-8,974.5	704.5	413.1
781.1	-11,391.5	101,309.2	-442,977.7	692,635.8	-398,893.5	66,437.9	-8,784.7	921.4
-255.9	1,544.8	-11,953.8	85,401.3	-398,893.5	577,684.1	-314,059.8	67,904.7	-7,469.7
-76.5	-90.1	1,577.8	-8,974.5	66,437.9	-314,059.8	483,996.3	-283,182.5	54,337.7
941.6	-1,624.5	1,145.4	704.5	-8,784.7	67,904.7	-283,182.5	388,592.3	-165,575.2
-421.2	986.1	-854.3	413.1	921.4	-7,469.7	54,337.7	-165,575.2	117,540.4

The mass matrix, assuming the first degree of freedom is at the bottom of the building, can thus be written:

**Table 7.1-7 Mass matrix of the regular nine-story building [tons]**

505	0	0	0	0	0	0	0	0
0	494.5	0	0	0	0	0	0	0
0	0	494.5	0	0	0	0	0	0
0	0	0	494.5	0	0	0	0	0
0	0	0	0	494.5	0	0	0	0
0	0	0	0	0	494.5	0	0	0
0	0	0	0	0	0	494.5	0	0
0	0	0	0	0	0	0	494.5	0
0	0	0	0	0	0	0	0	535

**7.1.3 Irregular building**

The irregular building is a modification of the shape of the original nine-story one. In particular it has been chosen to reduce the size of the last six floors. As a result, in correspondence of the third floor there is a significant vertical discontinuity. The vertical scheme is shown in Figure 7.1-2.

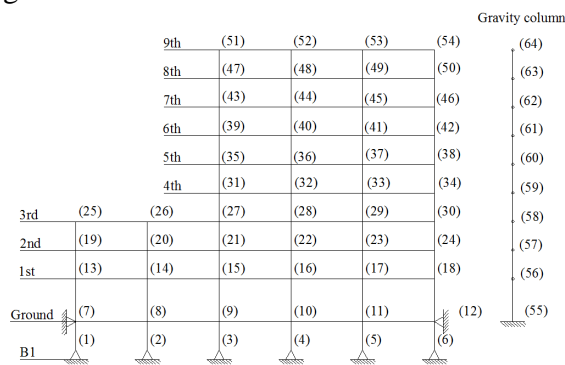


**Figure 7.1-1 Elevation view**

The seismic masses and loads are computed in the same way of the regular structure.

Table 7.1-1 Seismic weights for the irregular structure in [kN]

Node	X-	Y-	Node	X-	Y-	Node	X-	Y-	Node	X-	Y-
1	0.0	0.0	19	0.0	97.0	37	0	193.962	55	0	0
2	0.0	0.0	20	0.0	194.0	38	0	96.9813	56	4952.03	3961.62
3	0.0	0.0	21	0.0	194.0	39	0	96.9813	57	4849.06	3879.25
4	0.0	0.0	22	0.0	194.0	40	0	193.962	58	4849.06	3879.25
5	0.0	0.0	23	0.0	194.0	41	0	193.962	59	2909.44	2560.30
6	0.0	0.0	24	0.0	97.0	42	0	96.9813	60	2909.44	2560.30
7	0.0	96.5	25	0.0	97.0	43	0	96.9813	61	2909.44	2560.30
8	0.0	193.0	26	0.0	194.0	44	0	193.962	62	2909.44	2560.30
9	0.0	193.0	27	0.0	194.0	45	0	193.962	63	2909.44	2560.30
10	0.0	193.0	28	0.0	194.0	46	0	96.9813	64	3147.72	2769.99
11	0.0	193.0	29	0.0	194.0	47	0	96.9813			
12	0.0	96.5	30	0.0	97.0	48	0	193.962			
13	0.0	99.0	31	0.0	97.0	49	0	193.962			
14	0.0	198.1	32	0.0	194.0	50	0	96.9813			
15	0.0	198.1	33	0.0	194.0	51	0	96.9813			
16	0.0	198.1	34	0.0	97.0	52	0	193.962			
17	0.0	198.1	35	0.0	97.0	53	0	193.962			
18	0.0	99.0	36	0.0	194.0	54	0	96.9813			

Table 7.1-2 Static loads in [kN]

Node ID	Y-load	Node ID	Y-load	Node ID	Y-load	Node ID	Y-load
1	0.0	19	-97.0	37	-193.96	55	0
2	0.0	20	-194.0	38	-96.98	56	-9109.59
3	0.0	21	-194.0	39	-96.98	57	-8920.19
4	0.0	22	-194.0	40	-193.96	58	-8920.19
5	0.0	23	-194.0	41	-193.96	59	-5584.87
6	0.0	24	-97.0	42	-96.98	60	-5584.87
7	-99.0	25	-97.0	43	-96.98	61	-5584.87
8	-198.1	26	-194.0	44	-193.96	62	-5584.87
9	-198.1	27	-194.0	45	-193.96	63	-5584.87
10	-198.1	28	-194.0	46	-96.98	64	-6223.58
11	-198.1	29	-194.0	47	-96.98		
12	-99.0	30	-97.0	48	-193.96		
13	-97.0	31	-97.0	49	-193.96		
14	-194.0	32	-194.0	50	-96.98		
15	-194.0	33	-194.0	51	-96.98		
16	-194.0	34	-97.0	52	-193.96		
17	-194.0	35	-97.0	53	-193.96		
18	-97.0	36	-194.0	54	-96.98		

The stiffness matrix computed using the force method is shown below.

**Table 7.1-3 Stiffness matrix of the irregular building**

702,214.9	-559,555.2	113,250.4	-10,978.3	1,854.9	105.6	-105.9	-355.9	295.8
-559,555.2	922,704.8	-511,175.3	82,403.9	-10,843.0	1,155.7	128.0	398.4	-325.9
113,250.4	-511,175.3	693,985.7	-352,622.7	73,394.1	-9,706.5	1,426.1	-513.4	374.9
-10,978.3	82,403.9	-352,622.7	521,641.5	-296,236.9	60,960.4	-7,338.0	1,583.0	-327.2
1,854.9	-10,843.0	73,394.1	-296,236.9	455,558.3	-264,589.1	46,755.8	-6,573.7	878.2
105.6	1,155.7	-9,706.5	60,960.4	-264,589.1	379,098.7	-208,577.9	46,762.6	-5,214.4
-105.9	128.0	1,426.1	-7,338.0	46,755.8	-208,577.9	318,056.4	-187,251.5	36,864.0
-355.9	398.4	-513.4	1,583.0	-6,573.7	46,762.6	-187,251.5	253,168.6	-107,253.5
295.8	-325.9	374.9	-327.2	878.2	-5,214.4	36,864.0	-107,253.5	74,711.2

The mass matrix, assuming the first degree of freedom is at the bottom of the building, can thus be written:

**Table 7.1-4 Mass matrix of the irregular nine-story building [tons]**

505.00	0	0	0	0	0	0	0	0
0	494.50	0	0	0	0	0	0	0
0	0	494.50	0	0	0	0	0	0
0	0	0	296.70	0	0	0	0	0
0	0	0	0	296.70	0	0	0	0
0	0	0	0	0	296.70	0	0	0
0	0	0	0	0	0	296.70	0	0
0	0	0	0	0	0	0	296.70	0
0	0	0	0	0	0	0	0	321.00

## ***7.2 Allowable values for performance indices***

### ***7.2.1 Inter-story drift***

As already said inter-story drifts are chosen as performance indices for linear analysis due to they are representative of both structural and non-structural damage. The evaluation of the allowable values of these indices can be made in two ways.

The most formal procedure consists in estimating the inter-story drift which causes the formation of the first plastic hinge at the considered floor. In order to do that two forces must be applied to neighbor floors, and their intensity must be increased until the first element achieves inelastic behavior.



In case of lower performance levels the forces are increased until the unwanted effects occur (for example the formation of plastic hinges in columns can be considered). Although this way is computationally long and complicated.

**Table 7.2-1 Building Performance Levels**

<b>Table C1-8 Target Building Performance Levels and Ranges</b>						
<b>Structural Performance Levels and Ranges</b>						
<b>Nonstructural Performance Levels</b>	S-1 Immediate Occupancy	S-2 Damage Control Range	S-3 Life Safety	S-4 Limited Safety Range	S-5 Collapse Prevention	S-6 Not Considered
N-A Operational	Operational 1-A	2-A	Not recommended	Not recommended	Not recommended	Not recommended
N-B Immediate Occupancy	Immediate Occupancy 1-B	2-B	3-B	Not recommended	Not recommended	Not recommended
N-C Life Safety	1-C	2-C	Life Safety 3-C	4-C	5-C	6-C
N-D Hazards Reduced	Not recommended	2-D	3-D	4-D	5-D	6-D
N-E Not Considered	Not recommended	Not recommended	Not recommended	4-E	Collapse Prevention 5-E	No rehabilitation

A more practical solution is provided by codes. FEMA 356 – *Prestandard and Commentary for the Seismic Rehabilitation of Buildings* developed by the Federal Emergency Management Agency has been chosen. A so called Building Performance Level must be evaluated as the combination of a Structural Performance Level and a Nonstructural Performance Level which represent the level of damage that the structure can afford. There are six and five levels for respectively the structural and nonstructural performance ranges and one of them must be selected according to the importance of the building and to the requests of the building owner. Table 7.2-1 shows the different Performance Levels that can be adopted.

According to the selected Building Performance Level different acceptance criteria must be satisfied. In case of structural performance an approximate indication of an allowable value of inter-story drift is given in Table 7.2-2. As written in the code, these values serve to illustrate only typical overall structural response, and do not replace the limit given by the deformations of the singular members. Although, since the aim of the present research is a comparison of the efficiency of different methods, the proposed quantities are taken as reference. In particular a performance in between the Immediate Occupancy and the Life Safety levels was selected resulting in an allowable inter-story drift ratio of 1%.

**Table 7.2-2 Structural Performance Levels**

Steel Moment Frames	Primary	Extensive distortion of beams and column panels. Many fractures at moment connections, but shear connections remain intact.	Hinges form. Local buckling of some beam elements. Severe joint distortion; isolated moment connection fractures, but shear connections remain intact. A few elements may experience partial fracture.	Minor local yielding at a few places. No fractures. Minor buckling or observable permanent distortion of members.
	Secondary	Same as primary.	Extensive distortion of beams and column panels. Many fractures at moment connections, but shear connections remain intact.	Same as primary.
	Drift	5% transient or permanent	2.5% transient; 1% permanent	0.7% transient; negligible permanent

For what concern nonstructural damage the acceptance criteria depend on the technical requirements of the nonstructural components taken into account and for this reason is not considered here.

### 7.3 Seismic hazard

#### 7.3.1 Acceleration time-histories

There are two main possibilities to obtain acceleration time-histories. The first is to develop them from design acceleration response spectra for the considered geological location. The second is to exploit existing accelerograms relative to the same geological area, scaling them according to their possibility of exceedence.

In the present thesis the set of ground motions developed by the System Performance Team, Woodward-Clyde Federal Services of Pasadena, California for the SAC project has been chosen. The data files are available at the following webpage:

“[http://nisee.berkeley.edu/data/strong\\_motion/sacsteel/ground\\_motions.html](http://nisee.berkeley.edu/data/strong_motion/sacsteel/ground_motions.html)”

These acceleration time-histories include both records from historic earthquakes as well as artificially-generated time histories. The set relative to Los Angeles with a probability of exceedence of 10% in 50 years is considered. This ensemble is composed of twenty time-histories having the characteristics summarized in Table 7.3-1.

**Table 7.3-1 Details of Los Angeles ground motions having a possibility of exceedence of 10% in 50 years**

SAC Name	Record	Earthquake Magnitude	Scale Factor	DT (sec)	Duration (sec)	PGA (cm/sec <sup>2</sup> )
LA01	Imperial Valley, 1940, El Centro	6.9	2.01	0.02	39.38	452.03
LA02	Imperial Valley, 1940, El Centro	6.9	2.01	0.02	39.38	662.88
LA03	Imperial Valley, 1979, Array #05	6.5	1.01	0.01	39.38	386.04
LA04	Imperial Valley, 1979, Array #05	6.5	1.01	0.01	39.38	478.65

LA05	Imperial Valley, 1979, Array #06	6.5	0.84	0.01	39.08	295.69
LA06	Imperial Valley, 1979, Array #06	6.5	0.84	0.01	39.08	230.08
LA07	Landers, 1992, Barstow	7.3	3.2	0.02	79.98	412.98
LA08	Landers, 1992, Barstow	7.3	3.2	0.02	79.98	417.49
LA09	Landers, 1992, Yermo	7.3	2.17	0.02	79.98	509.7
LA10	Landers, 1992, Yermo	7.3	2.17	0.02	79.98	353.35
LA11	Loma Prieta, 1989, Gilroy	7	1.79	0.02	39.98	652.49
LA12	Loma Prieta, 1989, Gilroy	7	1.79	0.02	39.98	950.93
LA13	Northridge, 1994, Newhall	6.7	1.03	0.02	59.98	664.93
LA14	Northridge, 1994, Newhall	6.7	1.03	0.02	59.98	644.49
LA15	Northridge, 1994, Rinaldi RS	6.7	0.79	0.005	14.945	523.3
LA16	Northridge, 1994, Rinaldi RS	6.7	0.79	0.005	14.945	568.58
LA17	Northridge, 1994, Sylmar	6.7	0.99	0.02	59.98	558.43
LA18	Northridge, 1994, Sylmar	6.7	0.99	0.02	59.98	801.44
LA19	North Palm Springs, 1986	6	2.97	0.02	59.98	999.43
LA20	North Palm Springs, 1986	6	2.97	0.02	59.98	967.61

Since the effects of several seismic excitations must be superposed at each iteration it is suggested to find the so called “active ground motions”, that is the ground motions that produces the higher damage on the considered structure for different values of added damping. In order to do that a singular degree of freedom system having the same period of the first mode of the building is considered. Its damping ratio is increased until realistic values, i.e. 40%, and the maximum value of inter-story drift is registered for each ground motion. Figure 7.3-1 depicts the obtained results.

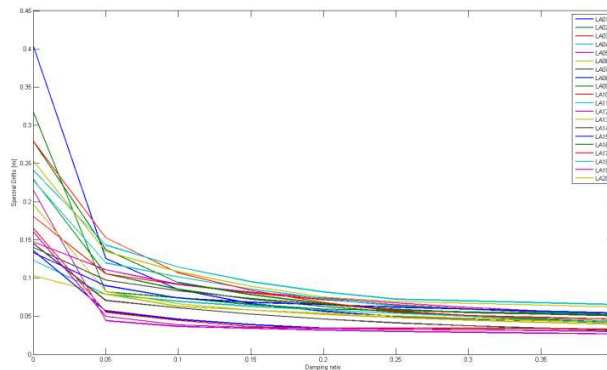


Figure 7.3-1 Spectral displacements vs damping ratio for a SDOF system with period 2.16 s

As can be seen, for the present structure the active ground motions are *LA01*, *LA11* and *LA18*. Analysis-redesign time-history and the simplified sequential search algorithm using drifts are then run using only these selected records. Then their resulting configurations are verified for all the other accelerograms. If the previous level of damage is exceeded for some acceleration time-history, then this record is added to the active list and the design is repeated. The main advantage is that usually not many

records are added and the time necessary to carry on the procedure decreases considerably.

### 7.3.2 Acceleration power spectral density

As seen in Annex A.4.6 the power spectral density relative to ground motions acceleration can be derived from the Fourier transform of the acceleration time-history of the records. Since the accelerograms are discrete functions, their frequency content has been computed using the Fast Fourier Transform. Then the obtained values can be interpolated with the spectrum functions given by Kanai-Tajimi or Clough-Penzien.

Theoretically one of these functions is needed for each record and then the envelope of the response power spectral density must be considered, like in the case of the time-history analysis-redesign. Although, due to the low influence on the response, as shown in chapter 5.4, it has been decided to interpolate the mean values of all the Fourier transform of the records. Moreover, since the set of ground motions is relative to a specific site, its spectral characteristics do not change significantly from one to another record. In this way only the parameters of one spectral function has been derived, simplifying the procedure. In Figure 7.3-1 the normalized mean values of the Fourier transform relative to the ground acceleration for the LA 10% in 50 years ensemble are shown.

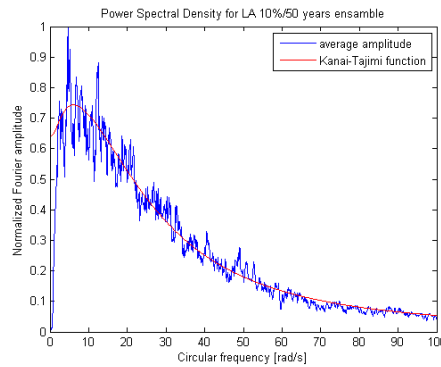


**Figure 7.3-1 Fitting of mean values of LA10 in 50 years ensemble with Kanai-Tajimi function**

The values are fitted using Kanai-Tajimi function:

$$S_{KT}(\bar{\omega}) = \frac{1 + 4\xi^2 \left(\frac{\bar{\omega}}{\omega_n}\right)^2}{\left(1 - \left(\frac{\bar{\omega}}{\omega_n}\right)^2\right)^2 + 4\xi^2 \left(\frac{\bar{\omega}}{\omega_n}\right)^2} S_0$$

where  $\xi = 1.5$ ,  $\omega_n = 10 \text{ rad/s}$  and  $S_0 = 0.64 \text{ m/s}^2$

## 7.4 Linear comparison

### 7.4.1 General procedure

Time-history analysis-redesign method is the only one that provides a measure for the total added damping necessary to achieve a given performance. For this reason this method is firstly run and the resulting damping is used for all the other procedures that need a value of total damping.

Drifts and damper forces are computed for each ground motion separately and their maximal values are then tabulated. Configurations of dampers and maximal drifts are finally presented.

### Time-history analysis-redesign

As explained before the ensemble relative to the Los Angeles ground motions with probability of exceedence of 10% in 50 years is considered. The allowable values of inter-story drifts are taken as the 1% of the story height that means 3.96 cm for all the floors except for the first one where the allowable value is equal to 5.49 cm.

Initial value of uniform damping, according to chapter 4.2.5, is taken equal to 2,055.7 kNs/m considering a damping ratio of 0.7.

The convergence of the objective function is quite fast and, as depicted in Figure 7.4-1 Objective function in the iterative process, its final value can be considered stable after ten iterations.

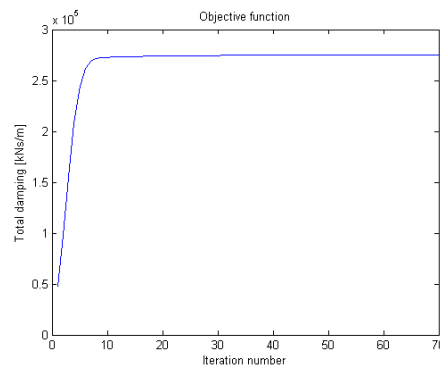


**Figure 7.4-1** Objective function in the iterative process

The final optimal added damping is equal to 275,300 kNs/m and is achieved after 70 iterations. Dampers are distributed at all floors except for the sixth and the ninth. In these story in fact, as can be seen in Figure 7.4-2 Final maximal drift, the maximal values of the performance index are lower than the allowable ones.

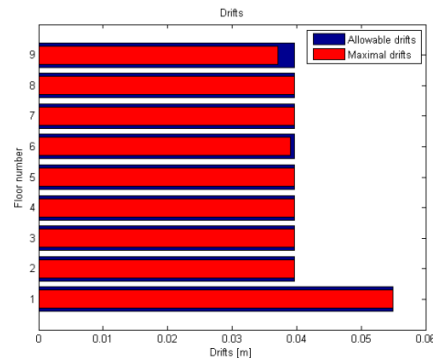


**Figure 7.4-2 Final maximal drift**

### Lyapunov-based analysis-redesign

Allowable values for the Lyapunov-based approach, as explained in chapter 4.9, are not connected with the real mean square values of inter-story drifts. Hence an inverse approach is adopted which means that the allowable quantities are changed until the desired amount of damping is achieved. In order to obtain a final added damping equal to the one obtained with the time-history analysis-redesign, i.e. 275,300 kNs/m, the root of the mean square values must be taken as 0.63743 times the allowable drifts used in time-history analysis-redesign.

Initial value of uniform damping, according to chapter 4.7.6, is taken equal to 2,055.7 kNs/m considering a damping ratio of 0.7. Also in this case the convergence is very fast and the value of added damping can be considered stable after only five iterations as can be seen in Figure 7.4-3 Objective function in the iterative process.

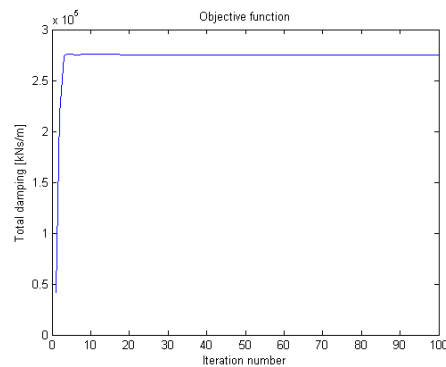


**Figure 7.4-3 Objective function in the iterative process**

### Linear Quadratic Regulator

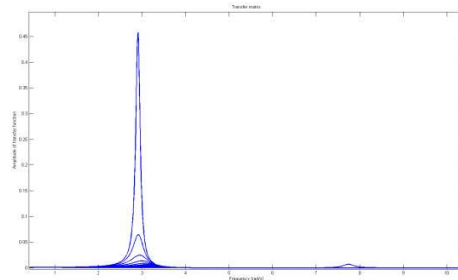
First mode approach is adopted in order to approximate the full matrix derived from Riccati's solution. The results obtained using a self-defined value of the parameter  $p$  were scaled as explained in chapter 3.2.4 to obtain the requested total added damping.

### Sequential Search Algorithm

The total amount of damping is divided into 200 increments to be sequentially placed along the structure.

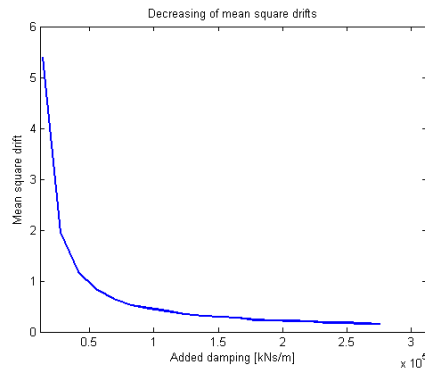
The seismic input is given in the form of power spectral density having the parameters  $\omega_n$  and  $S_0$  respectively equal to 1.5, 10 rad/s and 0.64 m/s<sup>2</sup> as explained in paragraph 7.3.2.

Figure 7.4-4 depicts the decreasing in the amplitude of the component relative to the first floor of the squared transfer matrix due to the added damping.



**Figure 7.4-4 Transfer matrix, component relative to the first floor**

Figure 7.4-5 shows the decreasing in the mean square drift relative to the first floor:



**Figure 7.4-5 Mean square drift amplitude of the first floor in the iterative process**

### *Simplified Sequential Search Algorithm*

The ensemble relative to the Los Angeles ground motions with probability of exceedence of 10% in 50 years is considered. The procedure is carried out using both inter-story velocities and drifts as performance indices.

The total added damping is divided into 100 increments to be sequentially placed along the structure.

### *Minimum transfer function*

As explained in chapter 6.2.3 the values of first order sensitivities trend to be similar as damping increases and it could be necessary to distribute the damping increment in more than one degree of freedom. In the implemented procedure the values of sensitivities are considered to be equal if their difference is less than 1%.

The total added damping is divided into 100 increments.



List of results

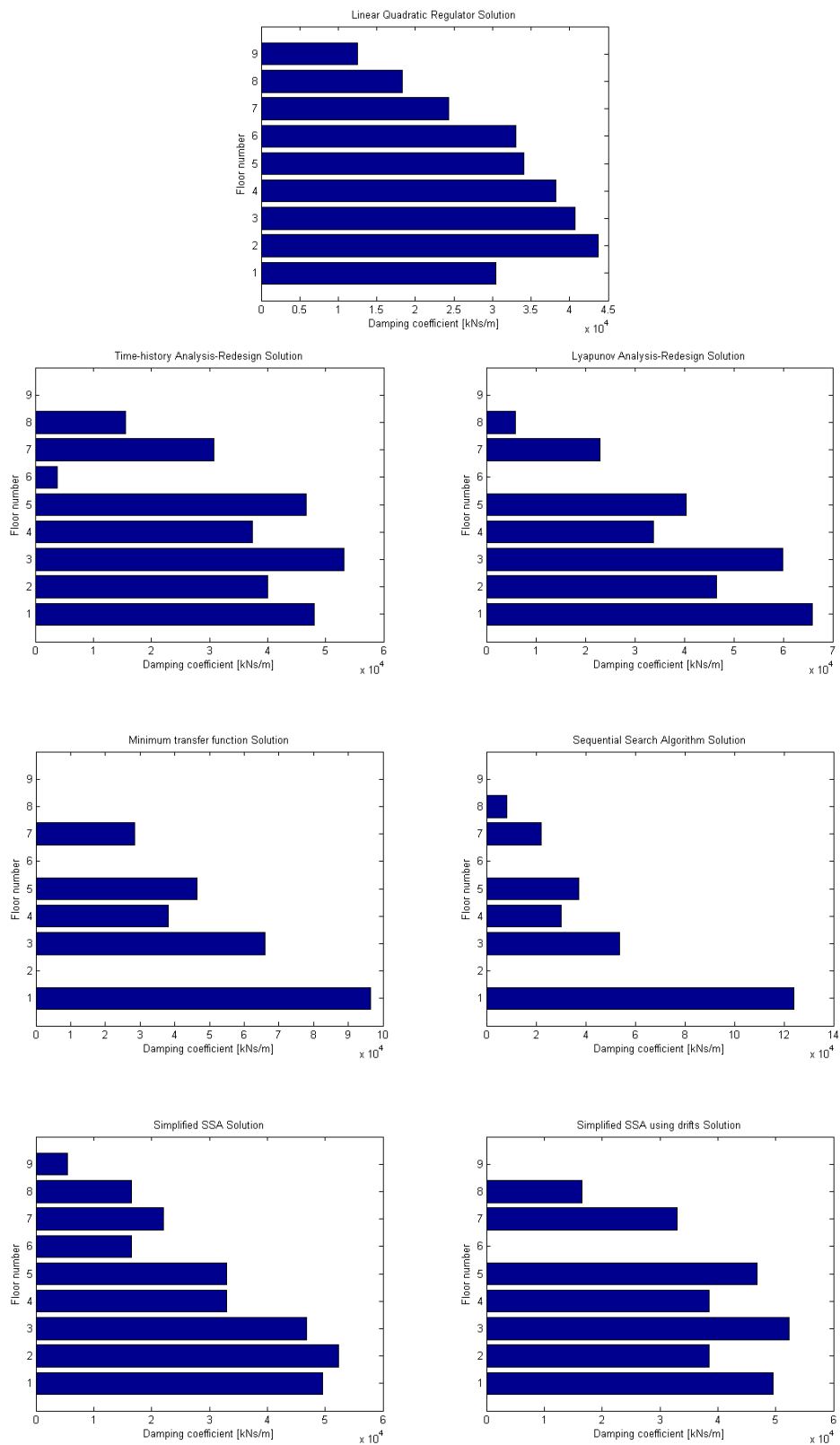
	<b>Linear Quadratic Regulator</b>		
Story number	Damper [kNs/m]	Max drift [%]	Max force [kN]
1	30,450	1.18	10,101
2	43,710	1.09	9,110
3	40,690	1.08	7,999
4	38,230	1.04	6,973
5	34,050	1.03	6,048
6	33,040	0.89	5,055
7	24,300	0.96	4,000
8	18,290	0.89	2,860
9	12,540	0.68	1,533
$\Sigma$	275,300	--	<b>53,679</b>
Max	--	<b>1.18</b>	<b>10,101</b>

	<b>Time-history analysis-</b>			<b>Lyapunov-based analysis-</b>		
Story number	Damper [kNs/m]	Max drift [%]	Max force [kN]	Damper [kNs/m]	Max drift [%]	Max force [kN]
1	48,030	1.00	12,737	65,840	0.87	13,839
2	40,000	1.00	8,358	46,490	0.92	8,824
3	53,090	1.00	9,778	59,870	0.98	10,747
4	37,370	1.00	6,759	33,800	1.03	6,865
5	46,630	1.00	8,053	40,420	1.08	8,410
6	3,850	0.98	798	0	1.10	0
7	30,710	1.00	5,689	23,020	1.20	5,599
8	15,610	1.00	3,146	5,860	1.33	1,651
9	0	0.94	0	0	1.19	0
$\Sigma$	275,290	--	<b>55,318</b>	275,300	--	<b>55,935</b>
Max	--	<b>1.00</b>	<b>12,737</b>	--	<b>1.33</b>	<b>13,839</b>

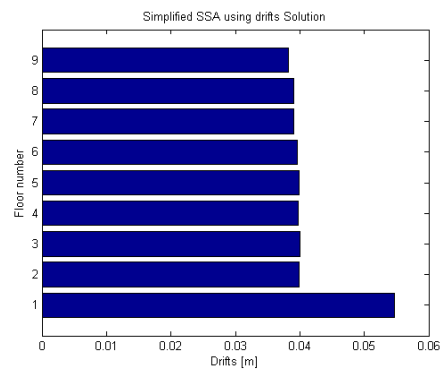
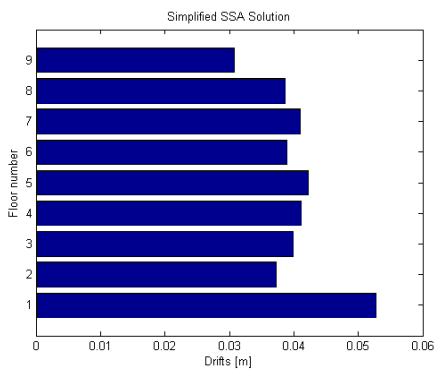
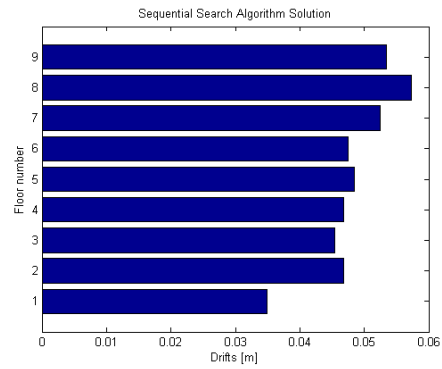
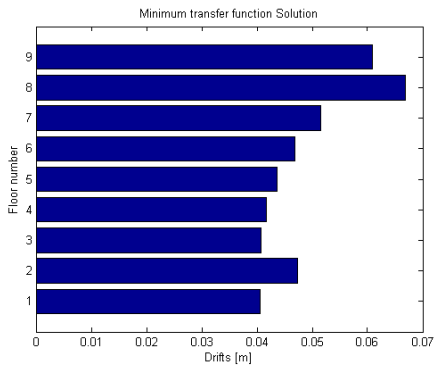
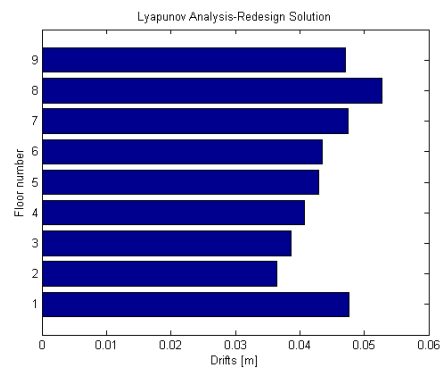
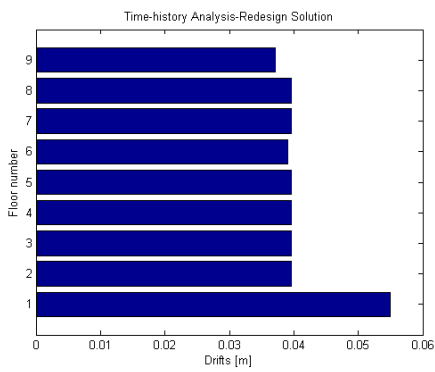
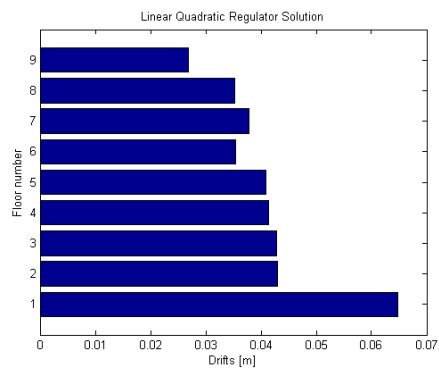
Story number	Simplified SSA			Simplified SSA using drifts		
	Damper [kNs/m]	Max drift [%]	Max force [kN]	Damper [kNs/m]	Max drift [%]	Max force
1	49,550	0.96	12,608	49,550	1.00	12,836
2	52,310	0.94	9,744	38,540	1.01	8,066
3	46,800	1.01	8,760	52,310	1.01	9,690
4	33,040	1.04	6,285	38,540	1.01	7,004
5	33,040	1.07	6,275	46,800	1.01	8,266
6	16,520	0.98	3,122	0	1.00	0
7	22,020	1.03	4,174	33,040	0.98	6,074
8	16,520	0.97	3,062	16,520	0.98	3,290
9	5,510	0.78	884	0	0.96	0
$\Sigma$	275,310	--	<b>54,914</b>	275,300	--	<b>55,226</b>
Max	--	<b>1.07</b>	<b>12,608</b>	--	<b>1.01</b>	<b>12,836</b>

Story number	Sequential Search Algorithm			Minimum transfer function		
	Damper [kNs/m]	Max drift [%]	Max force [kN]	Damper [kNs/m]	Max drift [%]	Max force [kN]
1	123,890	0.64	19,673	9,636	0.74	19,337
2	0	1.18	0	0	1.19	0
3	53,680	1.15	13,315	6,607	1.03	15,285
4	30,280	1.18	7,805	3,808	1.05	9,450
5	37,170	1.22	9,431	4,634	1.10	11,351
6	0	1.20	0	0	1.18	0
7	22,020	1.32	5,977	2,845	1.30	8,085
8	8,260	1.44	2,630	0	1.69	0
9	0	1.35	0	0	1.54	0
$\Sigma$	275,300	--	<b>58,831</b>	27,530	--	<b>63,508</b>
Max	--	<b>1.44</b>	<b>19,673</b>	--	<b>1.69</b>	<b>19,337</b>

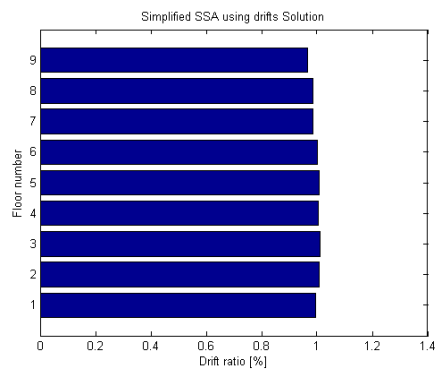
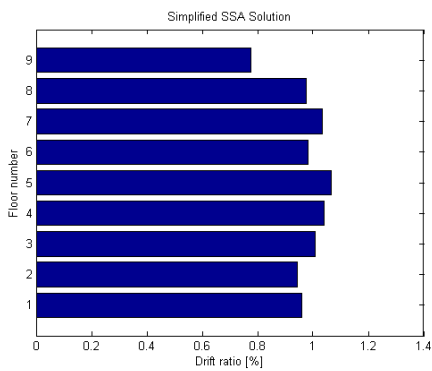
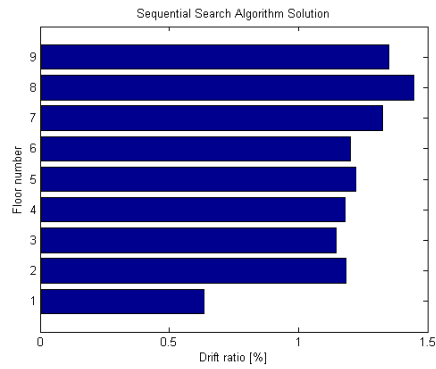
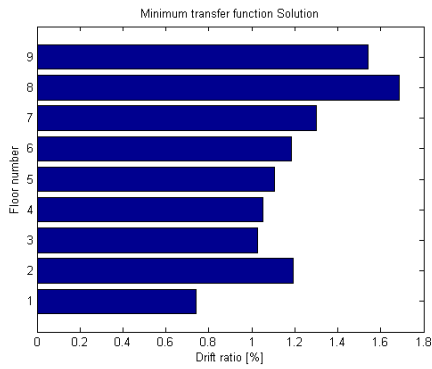
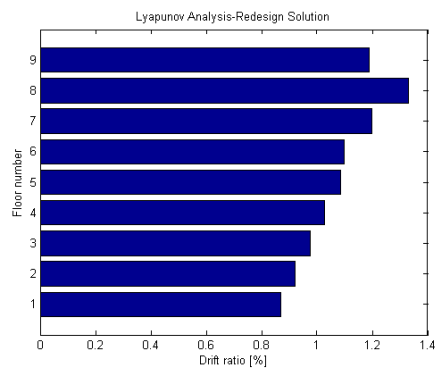
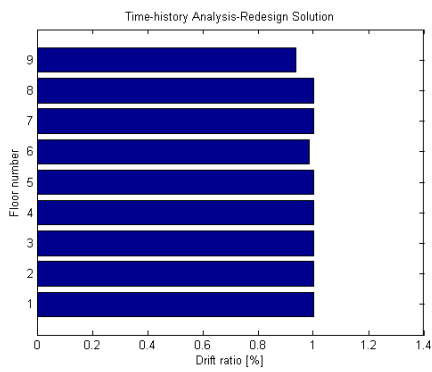
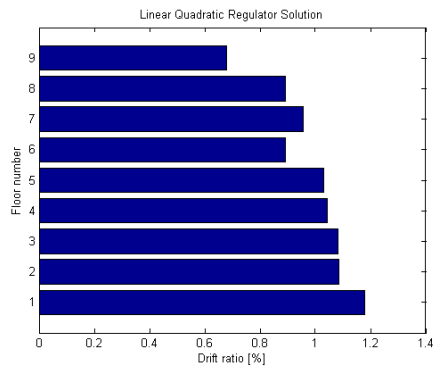
## Final damping configurations



## Maximal inter-story drifts



## Normalized inter-story drifts



### 7.4.2 Comparison

As can be seen by the graphs, the resulting configurations of dampers are really different each other. Three trends can be observed. A spread distribution, typical as already said of the linear quadratic regulator, is also present in the simplified sequential search algorithm. A concentration of damping in the first and in the central floors is instead present in the sequential search algorithm and in the minimum transfer function methods. In the case of the other methods the results show very similar configurations with a higher amount of damping at the bottom of the structure.

Riccati's solution presents, contrary to all other methods, a lower quantity of damping at the first floor which is the soft one. Despite this fact, the performances of this configuration are in good agreement with the results obtained from time-history analysis-redesign. The drift ratio at the first level in fact exceeds of only the 18% the reference value. This could be due to the particular type of structure here analyzed which requires a spread distribution of damping rather than a concentrate configuration.

The minimum transfer function method and the sequential search algorithm bring to configurations characterized by a large amount of damping in the first and in the third-fifth floors. Probably this is due to the fact that both this methods make use of frequency domain analysis to evaluate the optimal location index. On the other hand it is to note that the models of loading used in the two algorithms are really different. In the method developed by Takewaki only the first mode at the natural frequency of the system is considered, i.e. the input corresponds to a sinusoidal wave having frequency equal to the natural one of the structure. In case instead of the procedure of Zhang and Soong (1992) the input is modeled with a power spectral density function. Although, as noted in chapter 5.4, the modeling of this function as white noise or as a Kanai-Tajimi spectrum does not affect significantly the resulting configuration because of the predominance of the first mode. The predominance of the first mode also in the sequential search algorithm could be the reason of the similarity between the two methodologies. Their respective results show the trend to concentrate damping in correspondence to the soft parts of the structure: in the present case about the 25-30% of the total amount in the first floor. As a consequence the maximum drifts occur at the top floors exceeding the allowable drifts of the 40-60%.

Time-history analysis-redesign and simplified search algorithms achieve a really similar configuration, if the SSSA makes use of drifts as controllability indices rather than velocities. As can be seen from the graphs all the values of inter-story drifts are around 1% of the story height.

Finally Lyapunov-based analysis-redesign leads to results quite similar to the ones obtained from time-history procedures. The resulting drifts instead show a trend more similar to the frequency domain algorithms. Although, this could be due to the particular sensitivity of the present structure and it does not have general validity. Due to its low

computational cost, Lyapunov's solution represents an alternative to the heavier time-history analysis used in the simplified sequential search algorithm and in the time-history analysis-redesign.

The conclusions that can be made on the base of these results have not general validity because referred to a particular structure. Additional cases studies are necessary in order to provide more reliable results. Hence the considerations that follow concern only this particular type of structure.

It has been observed that the time-history analysis-redesign leads to the desired performance, i.e. enables performance based design, with minimum damping. Hence, its design was considered as a benchmark and the total amount of damping in other methods was chosen accordingly. The simplified sequential search algorithms, when modified to consider drift as the controllability index, provided very similar results in the example considered. Moreover, it could also be modified to lead to performance based designs if dampers are added until the desired performance is attained. The Lyapunov based analysis-redesign resulted in a similar damping distribution as the one attained by the time-history analysis-redesign. However, from some reason the resulted inter-story drifts were higher by up to 33%. This may be attributed to the sensitivity of the problem (combination of structure and ground motion ensemble) as other works indicated it could lead to comparable designs to those of the time-history analysis-redesign (Lavan and Levy (2009) and Levy and Lavan (2009)). The other methods that make use of frequency domain analysis tools also resulted in peak drifts larger than the allowed. Riccati's solution, the sequential search algorithm and Takewaki's methodology resulted in drifts 18%, 44% and 69% higher than the allowed, respectively. While those methods are expected to lead to higher drifts than the allowed, these could also be attributed to the sensitivity of the problem. It should be emphasized that some of these methods are based on the first mode response. This point could explain the high drifts the designs of these methods attained as the response of the structure at hand to the considered ground motions was also appreciably affected by the second mode. Note that in contrast to the time-history based methodologies, the methods that make use of frequency domain analyses cannot be used for performance based design, unless some reliable translation of performances from time domain (peak) to frequency domain (RMS), in each story separately, could be assessed. Also, an adequate stochastic representation of the seismic hazard should be used. In addition, those methodologies could not be easily modified to account for nonlinear behavior. It should be noted, on the other hand, that the computationally efficient tools associated with these methods, present an important advantage as time-history analysis is avoided.

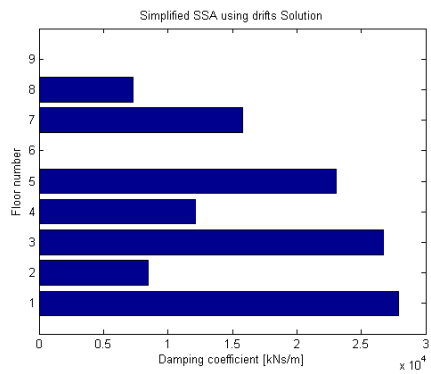
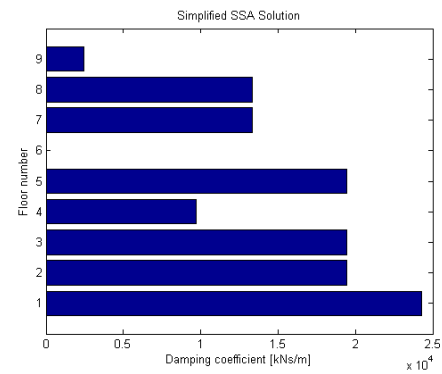
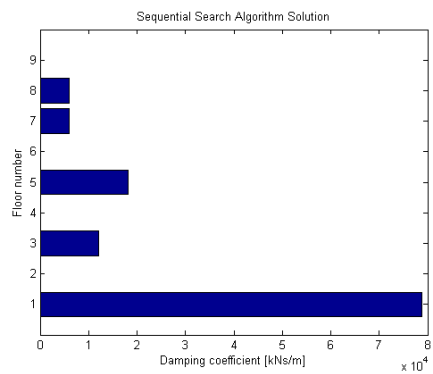
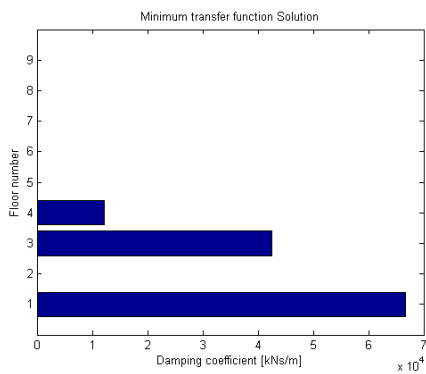
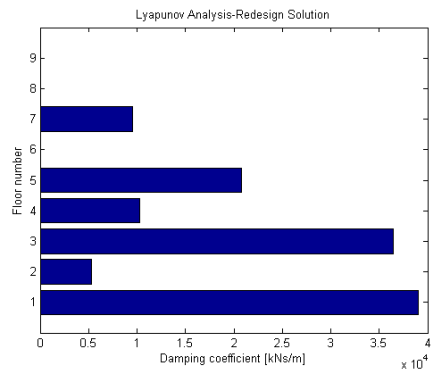
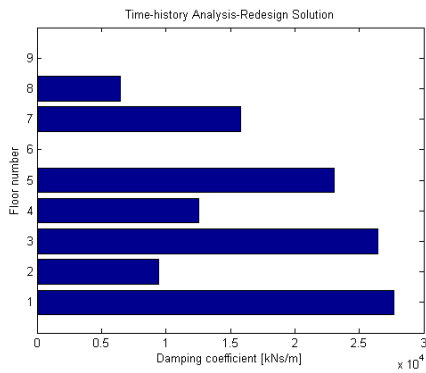
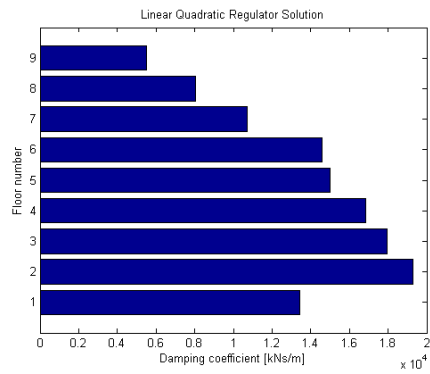
The results here presented are based on the value of total damping achieved considering the maximal values of the performance indices in the time-history analysis-redesign.

Seismic codes allow also considering the average values of performance indices in case more than eight ground motions are chosen. This is due to the fact that using a large number of records the effects of peak values relative to a particular accelerogram can be statistically neglected. In order to verify the existence of a dependency on these final configurations, the analyses are run based on the value of damping achieved using the average values of inter-story drifts in the time-history analysis-redesign. As can be seen from the graphs below, also if the deviation from the allowable value (1%) is lower, the general trend is the same that using peak values.

Note that in these latter analysis a total amount of damping of 121,370 kNs/m was estimated instead of the 275,300 kNs/m relative to the peak values.



## Final damping configurations



## Normalized inter-story drifts

